Hindawi
Journal of Sensors
Volume 2019, Article ID 2649809, 12 pages
https://doi.org/10.1155/2019/2649809

Research Article

Quality Assessment of Four DEMs Generated Using In-Track KOMPSAT-3 Stereo Images

Kwan-Young Oh, Kwang-Jae Lee, Eui-Cheom Jeong, and Youn-Soo Kim

Korea Aerospace Research Institute (KARI), Republic of Korea

Correspondence should be addressed to Kwang-Jae Lee; kjlee@kari.re.kr

Received 1 March 2019; Accepted 9 May 2019; Published 13 June 2019

Guest Editor: Lei Zhang

The purpose of this research was to analyze the quality and characteristics of four digital elevation models (DEMs) generated using in-track Korea Multi-Purpose Satellite (KOMPSAT)-3 stereo images. The sensor modeling methods were based on ground control points (GCPs), the initial rational polynomial coefficients (RPCs), relative adjustment, and the automatic bias-compensation method. The GCPs and check points (CPs) were extracted from the 0.25 m aerial orthoimage and the 5 m DEM provided by the National Geographic Information Institute (NGII). The DEMs had the same resolution as the reference DEM (5 m) and comparative analysis was carried out. The results indicate that when relative adjustment was applied alone (DEM 3), the percentage of matched points with a correlation of 0.8 or more was improved by at least 17% compared to the case where only initial RPCs were used (DEM 2). Although the absolute horizontal position error of DEM 3 could not be eliminated, the relative elevation error at the same position was reduced significantly. Therefore, if the relative positions of DEMs produced at different times can be corrected, they can be used for the detection of changes in altitude. When applying the automatic bias-compensation method (DEM 4) without GCPs, the percentage of matched points with a correlation of 0.8 or more was 70.1%. When GCPs were used (DEM 1), the value was 70.2%, i.e., almost identical to that of DEM 4. The mean difference in resolution among DEMs 1 and 4 was -1.8 ± 3.4 m (median, -1.0 m). The results show that DEMs of sufficient quality can be generated without GCPs. Furthermore, although discrepancies among the DEMs were noted in forest and shadow areas, it is possible to produce a 5~10 m resolution DEM by using additional image processing techniques, such as shadow removal.

1. Introduction

The Korea Multi-Purpose Satellite (KOMPSAT)-3 is a high-resolution optical satellite that was launched in May 2012. The panchromatic imagery provided by KOMPSAT-3 has a spatial resolution of 0.7 m and a swath width of around 16.8 km. Also, KOMPSAT-3 can acquire stereo images not only in cross-track form, but also in in-track form. Since the in-track stereo images acquire the area of interest (AOI) almost simultaneously, the geometry and radiometric conditions for DEM generation are very stable. Thus, by minimizing stereo matching error, a higher-quality digital elevation model (DEM) generation can be derived [1].

The DEM is essential in the field of remote sensing, and for acquiring geospatial information, and is typically generated based on stereo optical satellite imagery, radar interferometry, and laser scanning [2]. The global-scale Shuttle Radio Topography Mission (SRTM; radar), Advanced Spaceborne Thermal Emission and Reflection Radiometer (ASTER; optic), and Advanced Land Observing Satellite (ALOS; optic) DEMs, with 30 m resolution, are freely available. Multitemporal DEMs can provide valuable information for the study of dynamic phenomena, such as landslides and urban change [3]. This study aims to explore the potential utility of KOMPSAT-3 in-track stereo images for the generation of multitemporal DEMs. The availability of pre- and postevent DEMs can provide valuable information for studying dynamic phenomena.

The accuracy of DEMs generated using stereo images is largely dependent on two factors [4], the first of which is the accuracy of the sensor modeling. Typically, the bundle adjustment method of rational function models (RFMs) is used to establish the relationship between a satellite's image coordinates and the ground coordinates [5]. Second, DEM

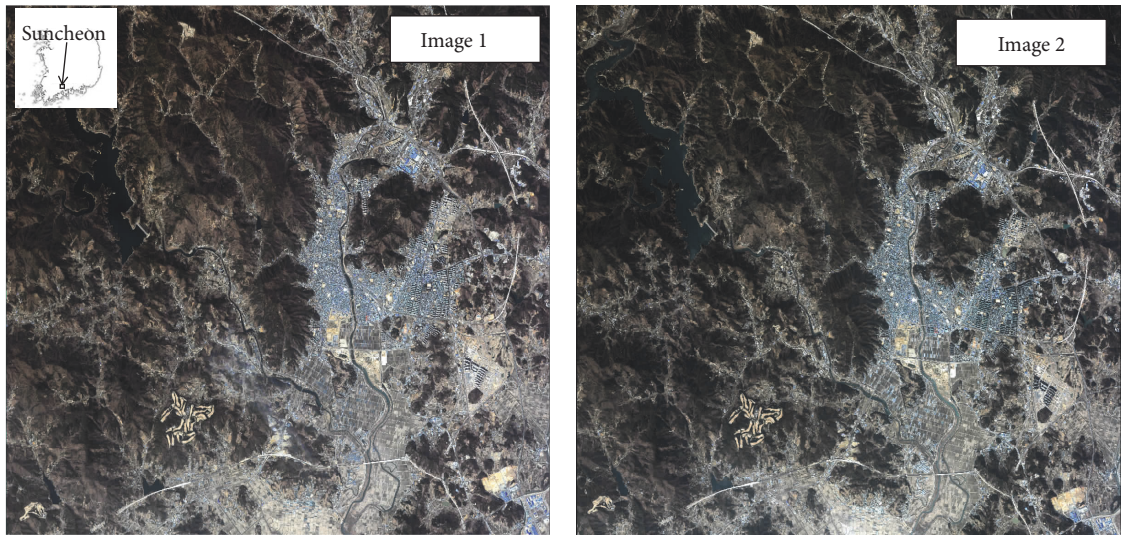

(a) (b)

Figure 1: Korea Multi-Purpose Satellite (KOMPSAT)-3 in-track stereo images: (a) forward image, (b) backward image.

accuracy depends on the stability of the stereo geometry. It is known that the closer the stereo geometry is to an isosceles triangle, the more accurate the three-dimensional (3D) positioning data is. To date, several studies have focused on the accuracy of sensor modeling. Oh et al. [6] analyzed the 3D positioning accuracy of KOMPSAT-2's stereo images with RFMs and found that, when using ground control points (GCPs), it could achieve horizontal and vertical accuracy of two or less pixels. Additionally, Lee et al. [7] predicted that errors in KOMPSAT-3 sensor modeling will not exceed 3 m, even when only one GCP is used. Furthermore, Oh et al. [8, 9] introduced an automatic bias-compensation method for the KOMPSAT series; when using the SRTM DEM as reference data, it achieved a sensor modeling accuracy of 10 m or less in the X, Y, and Z directions. Studies aimed at establishing the stability of stereo geometry have also been carried out: Jeong [4] analyzed the compatibility of stereo geometry data with the 3D positioning data of a stereo image pair, as generated by the same and different types of satellites, and showed that when the stereo geometry is unstable, the accuracy of 3D positioning accuracy of the stereo image pair may be reduced.

In this study, we compared the accuracy of four DEMs which were generated by four difference methods. First, we analyzed the stereo geometry of various KOMPSAT-3 in-track stereo images. Among them, stereo images with stably determined stereo geometry were selected for this study. Four DEMs were generated using GCP-based bundle adjustment, initial RPCs, relative adjustment, and automatic bias-compensation method. The accuracy of the generated DEMs was assessed by comparison with check points (CPs) and the National Geographic Information Institute (NGII) DEM. The GCPs and CPs were acquired using a combination of the NGII aerial orthoimage and the NGII DEM. The structure of this paper is as follows: in Section 2, we will discuss the reference data and study area. In Section 3, we will describe the methods used and the results. In Section 4, we will compare and assess the accuracy of generated DEMs by comparison to the NGII DEM (reference DEM). Finally, we will present conclusions in Section 5.

2. Study Area and Test Data

2.1. Study Area and KOMPSAT-3 Stereo Images. In this study, we used KOMPSAT-3 stereo images of Suncheon City, South Korea. The images were acquired between 13:32 and 13:34 PM (local time) on February 25, 2013; there was one forward and one backward image per pair (Figure 1). The data were acquired with single pass stereo imaging mode. The image product is a level 1R image, which was subjected to radiometric, but not geometric correction. The acquired image contained plains, lakes, mountains, and man-made structures, such as buildings, roads, and bridges.

Stereo geometry is determined by the location and attitude angle (roll, pitch, and yaw) of the satellite. The altitudes at which the stereo images were acquired were almost the same, at 699.6 and 699.3 km for the forward and backward images, respectively. The in-track forward and backward images have pitch angles of 14.2° and 13.8°, respectively. The spatial resolution is 0.7 m in the column direction and 0.8 m in the line direction, and the resolution of the latter is slightly lower. The satellite's altitude, altitude angle, and azimuth angle are used to calculate the stereo geometry, which affects the accuracy of the 3D positioning.

Figure 2 presents the ground point, satellite position vectors (left and right rays), and baseline, which together form the epipolar plane. The stability of the stereo geometry is determined by the epipolar plane. In other words, it is known that the accuracy of the three-dimensional position information increases with the stereo pair as it is closer to the shape of the isosceles triangle. It is known that the accuracy of 3D positioning information is enhanced by acquiring stereo images having epipolar plane close to an

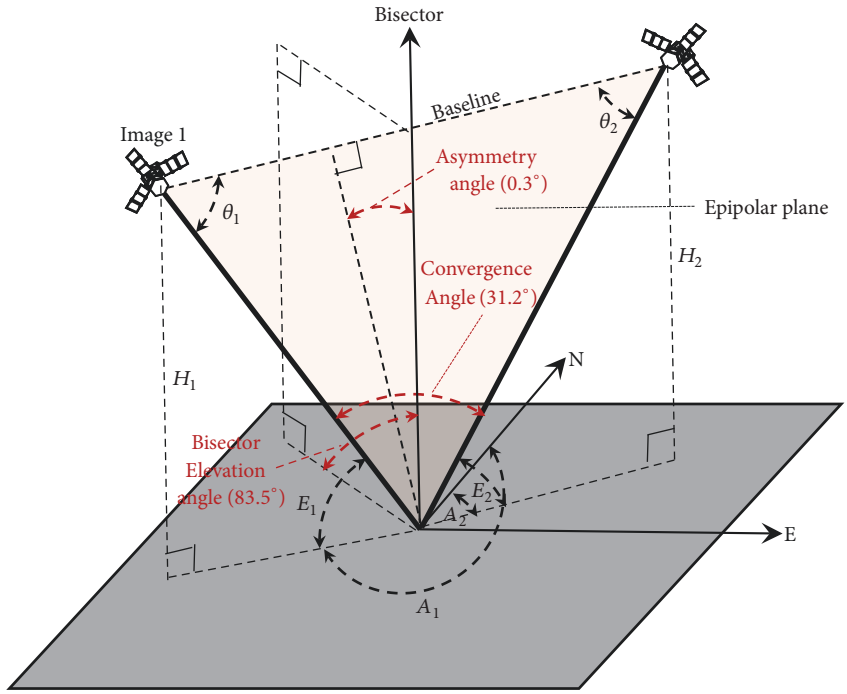

Figure 2: Stereo geometry.

Table 1: Specification of the KOMPSAT-3 in-track stereo image pair.

Characteristics	Forward	Backward
Product level	1R	
Acquisition time (UTC)	13:32:55 (local time), February 25, 2013	13:34:47 (local time), February 25, 2013
Satellite altitude (km)	699.9	699.3
Roll/pitch/yaw angle (deg.)	5.0/-14.2/-3.4	6.6/13.8/-3.0
Elevation angle (deg.)	73.5	72.8
Azimuth angle (deg.)	8.9	144.9
Pan image GSD (col./row)	0.7/0.8	0.7/0.8
Pan image size (col/row)	24060/20668	24060/20792
Image center coordinate (lat./long/)	34.945310730/ 127.470499034	34.947856143/ 127.470747229
Orbit type	Ascending orbit	

GSD, ground sample distance

isosceles triangle [10]. Typical stereo geometry parameters are the base-height (B/H) ratio, convergence angle, asymmetry angle, bisector elevation angle, and roll angle in the baseline direction (Figure 2). The stereo geometry parameters are shown in Figure 2 and Table 2, based on the information presented in Table 1. The convergence angle mainly affects the elevation precision; the convergence angles that are greater than 30° considerably enhance elevation precision for a given target. However, a convergence angle that is excessively large may cause a large geometric difference between the stereo images, thus lowering the stereo matching accuracy. The stereo images have an azimuth angle difference of around 136°; the forward and backward images form a stereo plane according to the flight direction of the satellite. The satellites are almost perpendicular to the ground surface, forming a bisector elevation angle of 83.5° and an epipolar plane (asymmetry angle, 0.3) close to an isosceles triangle. Thus, the stereo geometry is optimal.

2.2. Reference Data. We used a 0.25 m NGII orthoimage and a 5 m NGII DEM to evaluate the accuracy of sensor modeling and DEM (Figures 3(a), and 3(b)). Four GCPs and twelve CPs were obtained from the reference data and stereo images (Figure 4); these were used to calibrate the RFM model and evaluate the accuracy of the sensor modeling. Additionally, an SRTM DEM (single-arc) in Figure 3(c) was

Table 2: Stereo geometry parameters.

Characteristics	Parameter	Stable
B/H ratio	0.6	0.6-1.0
Convergence angle (deg.)	31.2	≥30 (deg.)
Asymmetry angle (deg.)	0.3	≤10 (deg.)
Bisector elevation angle (deg.)	83.5	≥70 (deg.)
Roll angle (baseline direction) (deg.)	0.1	≤10 (deg.)

B/H, base-height

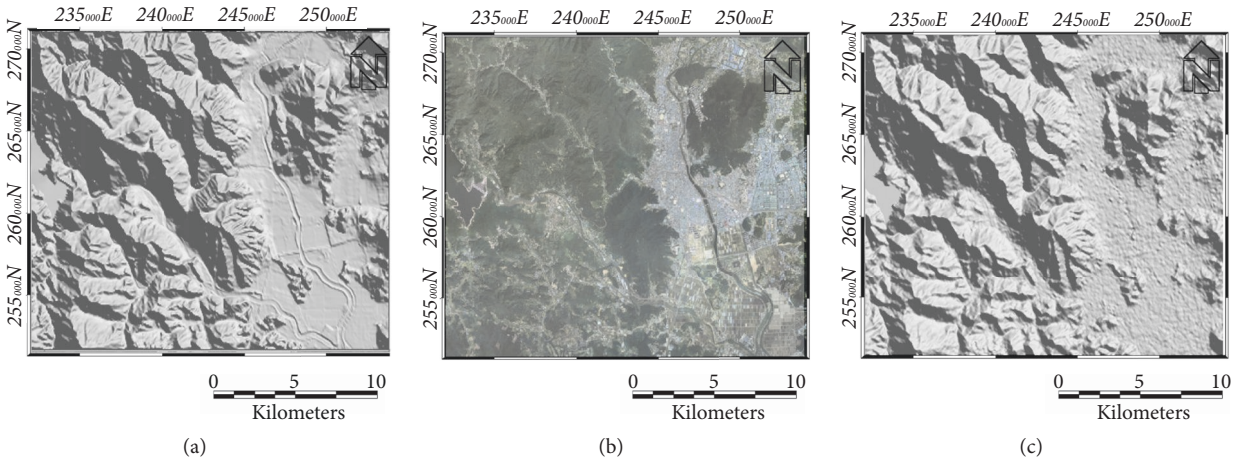

Figure 3: Reference data for (a) the National Geographic Information Institute (NGII) digital elevation model (DEM), (b) the NGII orthoimage, and (c) the Shuttle Radio Topography Mission (SRTM) DEM (single-arc).

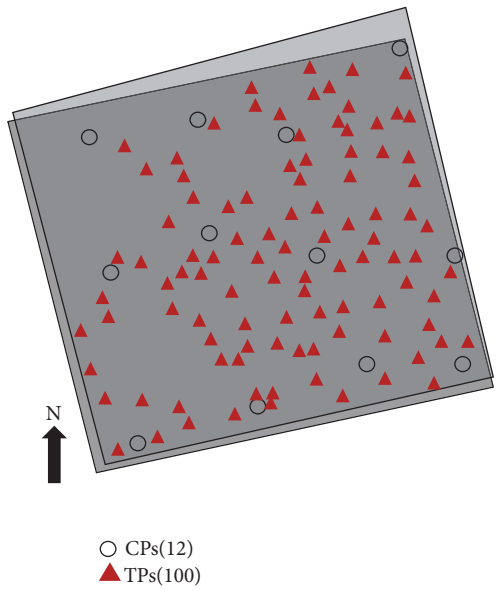

Figure 4: Distribution of ground control points (GCPs), check points (CPs) and tie points (TPs).

used for automated bias-compensation method [8]. In 2014, NGII tested the accuracy of the height data of their SRTM DEM and NGII DEM for the entire area of South Korea (Table 3). For the NGII DEM, the maximum and minimum height errors were -23.6 and 0 m, respectively. The mean, standard deviation, and mean square error were -0.7, 4.8, and 4.9 m, respectively. For the SRTM DEM, the maximum and minimum height errors were -21.4 and 0 m, respectively, and the mean, standard deviation, and mean square error were -3.0, 4.3, and 5.2 m, respectively. The mean root mean square error (RMSE) and standard deviation for both DEMs were less than 5 m. The maximum error of the NGII DEM was approximately 2 m larger than that of the SRTM DEM. However, the average error of the SRTM DEM was around four times higher than that of the NGII DEM.

Additionally, 100 tie points (TPs) were automatically extracted; these are used for data adjustment in the automatic bias-compensation method (Figure 4). Based on the corrected RFM model, DEMs with 5 m resolution were generated and compared to the reference DEM.

3. Method

The KOMPSAT-3 level 1R in-track stereo images were used to generate the DEMs in this study. Image-matching was performed using the pan band. The grid size was 5 m, in accordance with the ground sample distance (GSD) of the reference DEM. The RPCs were used to transform the images and geographic (lat./long.) coordinates [11]. The RPCs are supplied with each image so that image coordinates can be derived using (1) and (2), where X_n, Y_n, and Z_n are the normalized longitude, latitude, and height of the ground

Table 3: Reference data parameters (from the NGII [10]).

Reference data		NGII DEM	NGII orthoimage	SRTM DEM (single-arc)
Projection			Transverse Mercator	
Spheroid datum			GRS 1980	
Central datum			N 38°00′00″, E 127°00′00″	
GSD (m)		5	0.25	30
Horizontal error (m)		≤10	≤0.5	≤12.6
Height error	RMSE (m)	4.9	-	5.2
	Min/max (m)	-23.6/0	-	-21.4/0
	Mean/SD (m)	-0.7/4.8	-	-3.0/4.3

GSD, ground sample distance; RMSE, root mean square error; SD, standard deviation; NGII, National Geographic Information Institute; DEM, digital elevation model; STRM, Shuttle Radio Topography Mission; GRS, Geodetic Reference System

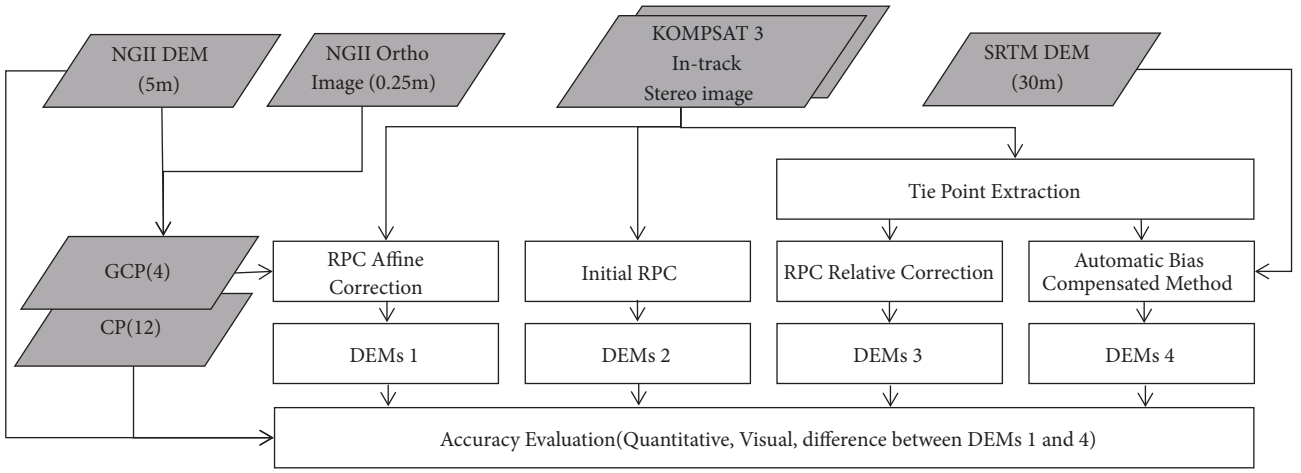

Figure 5: Flowchart of the study.

coordinates, respectively; l_n, and s_n are the normalized line (row) and sample (column) image coordinates, respectively; and $p1$, $p2$, $p3$, and $p4$ are rational functions composed of a numerator and denominator, having a 20-term cubic form. If the left and right image coordinates of a given TPs are known for a stereo image pair, the corresponding ground coordinates can be calculated using the least-squares method via inverse transformation:

$$l_n = \frac{p1\,(X_n, Y_n, Z_n)}{p2\,(X_n, Y_n, Z_n)} \quad (1)$$

$$s_n = \frac{p3\,(X_n, Y_n, Z_n)}{p4\,(X_n, Y_n, Z_n)} \quad (2)$$

However, there is typically a bias associated with the RPCs, due to the limited accuracy of the satellite orientation and ephemeris data; this bias must be compensated for so that the stereo images will be correctly matched. The RPC bias is usually corrected using GCPs. To correct the RPC bias, image coordinates were extracted from the stereo images. The ground coordinates of these points were estimated initially based on the first-order RPC coefficients. The RPC bias and ground position of the image points were then estimated using the RPC affine correction [12].

Figure 5 shows the process by which the four DEMs in this study were generated and their accuracy was evaluated. In DEM 1, RCP affine correction was applied using four GCPs. Through visual comparison of the stereo images with the NGII orthoimage, the image coordinates and horizontal coordinate were acquired for the CPs/GCPs. Additionally, the altitude of the horizontal coordinate was extracted from the NGII DEM. In DEM 2, the raw RPCs were used without any correction. In DEM 3, relative correction was applied [13]. Relative correction refers to the process wherein one image is defined as the base image and the RPCs of the overlapping images are then corrected with reference to this base image. To correct the RPCs bias, TPs were first automatically extracted using a hybrid matching method [14]. For relative correction, the ground coordinates of TPs are fixed at the values calculated using the raw RPCs. An RPC-based affine correction was used to correct the coordinates of the image calculated based on the raw RPCs, and the ground coordinates were applied to the image coordinates of the TPs. Finally, in DEM 4, the automatic bias-compensation method was applied using 100 TPs from the SRTM DEM and stereo images [6]. The initial ground coordinates of the 100 TPs, which are estimated using initial RPCs, have systematic errors. It may be assumed that these errors are large in absolute terms, but relatively small; that is, while

Table 4: Parameter values for image matching.

Stereo pair	Parameter
Projection	Transverse Mercator
Spheroid datum	GRS 1980
Image band (num.)	1 (pan)
GSD (m)	5
Search size (pixel)	21 x 3
Correlation size (pixel)	7 x 7
Correlation threshold	0.7

GSD, ground sample distance; GRS, Geodetic Reference System

errors in the initial ground coordinates of TPs may be large, the difference in error between adjacent TPs may be small. Based on this assumption, the initial ground coordinates of the TPs can be refined by matching the heights of the initial ground coordinates with those of the DEM [8, 9]. Through this process, the TPs are calibrated, in terms of their ground position, and then used as virtual GCPs.

The corrected RPCs were generated using the process applied in DEMs 1, 3, and 4. We also performed preprocessing for stereo matching, via epipolar image generation, using the corrected RPCs. Next, mass points were extracted via stereo matching, and filtering for elimination of excess error was performed to generate the DEM. For stereo matching, a hybrid matching method combining cross-correlation and least-squares matching was applied [14]. After sensor modeling, the DEMs were generated via automatic processes, with adjustment according to the parameter values presented in Table 4. The stereo matching was restricted to 12 × 3 pixels along the epipolar line, and the final 5 m DEM was created using the extracted mass points when the correlation threshold of 0.7 was exceeded. The final accuracy was assessed through comparison with the NGII DEM.

4. Results

4.1. Visual Analysis. Figure 6 compares the reference DEM (NGII DEM) with generated DEMs in this study. Figure 6(a) is the reference DEM, and Figure 6(b) is the DEM created by RPC affine correction with four GCPs. Overall, DEM 1 is not as smooth as the reference DEM, but it well describes topographical features such as buildings and forested areas. DEMs 2~4 (Figures 6(c)–6(e)) were generated without using GCPs. When the initial RPCs were used, DEM 2 showed a relatively poor performance in depicting some of the topographical features (Figure 6(c)). However, after relative correction had been performed, performance was improved significantly (Figure 6(d)) because the y parallax was minimized such that matching error was decreased [13]. Additionally, the automatic bias-compensation method applied in DEM 4 (Figure 6(c)) showed almost the same results as those obtained by RPC affine correction for DEM 1 (Figure 6(b)). With the exception of DEM 2 (Figure 6(c)), all DEMs (i.e., DEMs 1, 3, and 4) were similar to the reference DEM.

However, there were slight differences between the generated and reference DEMs in terms of areas where artificial or natural topographical features were distributed, such as urban areas and mountain areas. First, these differences could be due to differences in the methods used to generate DEMs and the reference DEM. The reference DEM was produced by interpolating contours from a digital topographic map of 1:5,000 scale while DEMs were produced based on ground point clouds obtained via space intersection of stereo RPCs, so that the object on the ground surface could be imaged accurately. Weighted filtering is applied based on standard deviation values to eliminate error; however, perfect removal of error is unlikely (see the urban area (region A) in Figure 6). Second, matching error caused by differences in spectral characteristics of the stereo images may have contributed to the slight differences between generated DEMs and the reference DEM. Particularly in mountainous areas with steep slopes, and in urban areas where shadow can occur, even if an accurate sensor modeling is used and stable stereo geometry is applied, stereo matching error is possible. Such problems can be seen in the expanded image in region B (i.e., the forested area) of Figure 6. Figure 7 shows hill-shade in the reference DEM and generated DEMs. Visual analysis showed that DEMs 1, 3, and 4 captured the hill-shade with similar accuracy to that of the reference DEM; however, generated DEMs showed significantly more noise.

4.2. Quantitative Analysis. Table 5 presents the sensor modeling accuracy of 12 CPs. In DEMs 2 and 3, the horizontal and vertical accuracies were highly similar. The value of the vertical accuracy parameter, the linear error at 90% (LE90), was 2.2 m for DEM 1, and that of the horizontal accuracy parameter, the circular error at 90% (CE90), was 1.0 m. According to the resolution of KOMPSAT-3, this is equivalent to an error of around 1~3 pixels, which likely corresponds to the error in the reference NGII DEM and NGII orthoimage (i.e., two or less pixels; see Table 3) from which the GCPs and CPs data were extracted. The LE90 value for DEM 4 was 4.5 m, while that of CE90 was 8.9 m. Although these values differed from those for DEM 1, DEM 4 showed an accuracy at least 12 times greater than that before any correction was applied.

Figure 8 shows the results of the mass points extraction, using the initial and calibrated RPCs, for all of DEMs. Correlations between the mass points were classified as Excellent (0.85~1.00), Good (0.7~0.85), or Fair (0.5~0.7). DEMs 1 and 4 showed similar 'Excellent' correlation rates, of 70.2% and 70.1%, respectively. When the initial RPCs were used (DEM 1), only 51.8% of mass points showed an 'Excellent' correlation. However, when relative correction was applied (DEM 2), this figure increased by approximately 18%, to 69.5. The 'Excellent' and 'Good' mass points were used as ground point clouds via space intersection of stereo RPCs. These point clouds were interpolated to 5 m resolution DEMs, as shown in Figures 6 and 7.

The elevation differences between DEMs 1 to 4 and the reference DEM are shown in Figure 9 and Table 6. When the initial RPCs were used (DEM 2), the RMSE was 29.8 m and the LE90 was 47.8 m; that is, around three times less

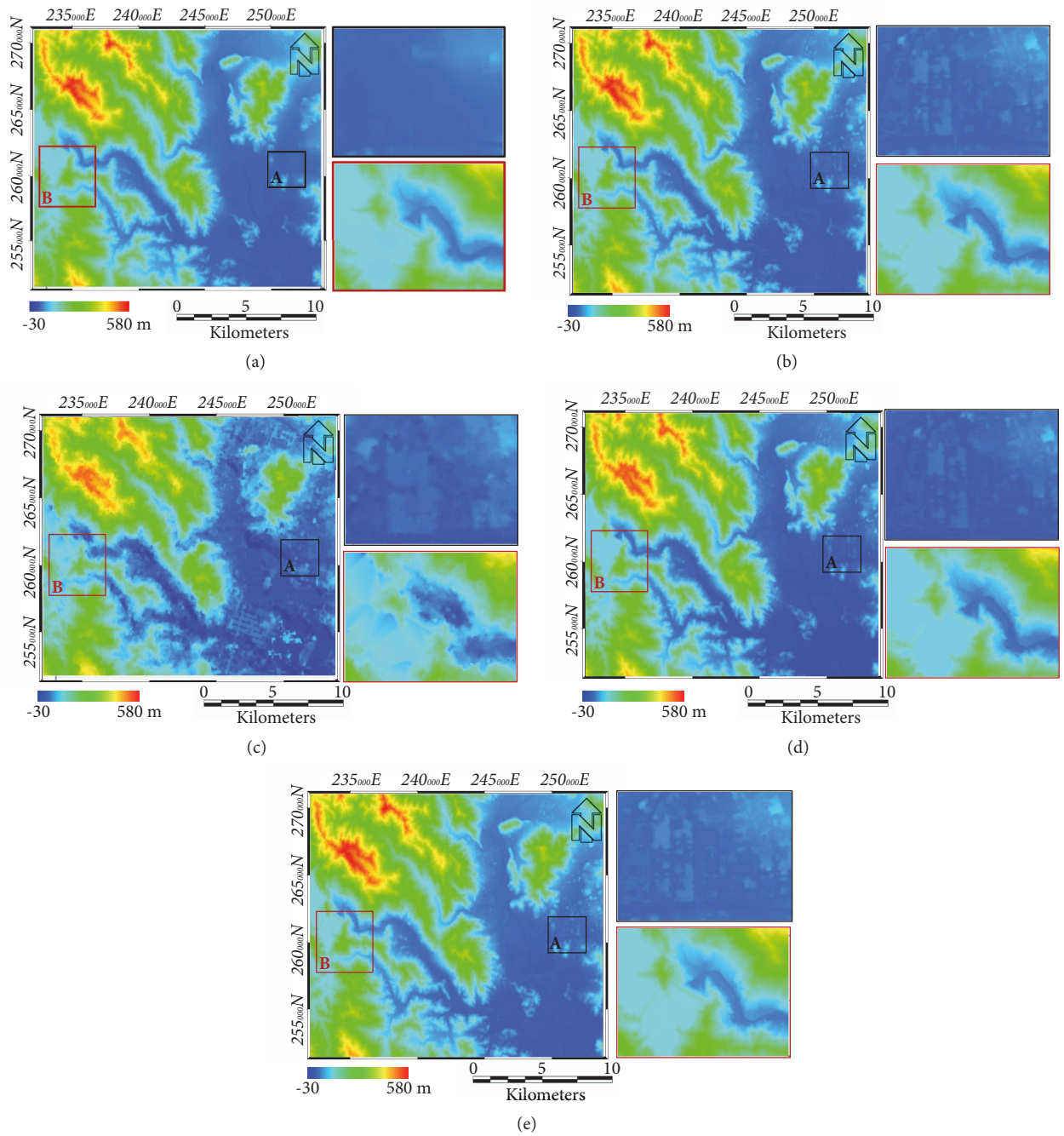

Figure 6: Comparison of the DEMs: (a) the reference DEM, (b) DEM 1, (c) DEM 2, (d) DEM 3, and (e) DEM 4.

Table 5: Sensor Modeling Accuracy of check point data.

Parameter		DEM 1	DEM 2	DEM 3	DEM 4
Vertical accuracy	Mean error (Z coordinate) (m)	-0.4	-8.9	-8.9	4.4
	RMSE (Z coordinate) (m)	1.4	10.4	10.4	5.9
	LE90 (m)	2.2	16.1	16.1	4.5
Horizontal accuracy	Mean error (X coordinate) (m)	-0.1	67.3	67.3	6.1
	RMSE (X coordinate) (m)	0.6	67.3	67.2	6.2
	Mean error (Y coordinate) (m)	-0.1	-93.2	-93.2	5.6
	RMSE (Y coordinate) (m)	0.4	93.2	93.2	5.6
	CE90 (m)	1.0	114.3	114.3	8.9

RMSE, root mean square; LE90, linear error at 90%; CE90, circular error at 90%

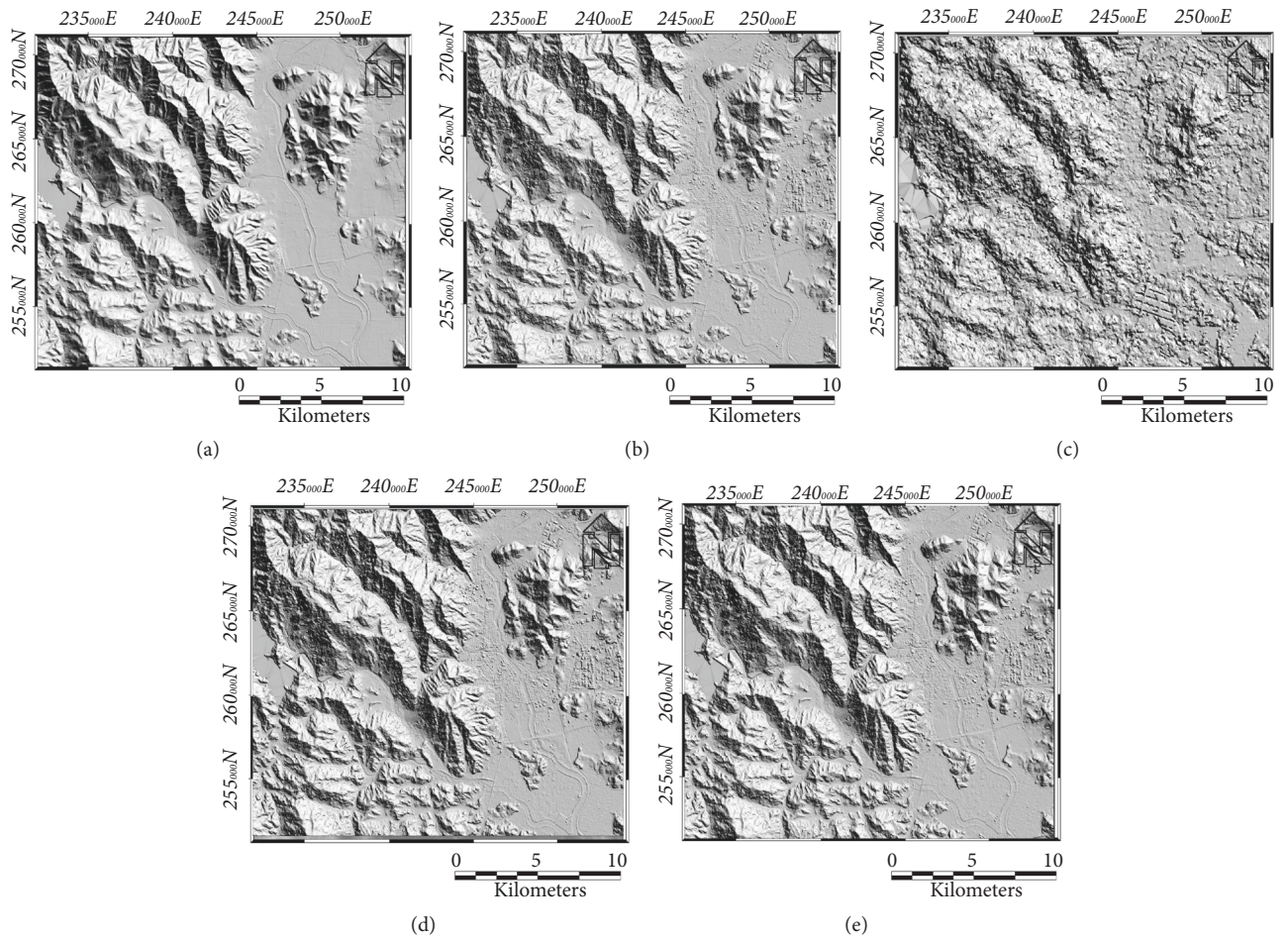

Figure 7: Hill-shade DEMs: (a) the reference DEM, (b) DEM 1, (c) DEM 2, (d) DEM 3, and (e) DEM 4.

Table 6: Accuracy of generated DEMs in this study.

Parameter		DEM 1	DEM 2	DEM 3	DEM 4
Vertical accuracy	Min error (m)	-36.7	-128.7	-113.5	-37.3
	Max error (m)	56.8	172.5	99.9	58.1
	Mean Error (m)	2.2	15.4	-3.8	5.6
	RMSE (m)	7.2	29.8	22.9	10.4
	LE90 (m)	12.6	47.8	38.7	18.4

accurate than the CPs-based estimation (Table 5). For DEM 3, however, the RMSE was improved (22.9 m). It is likely that the errors that occurred in the process of stereo matching were associated with y parallax reduction. Nevertheless, through this process, stereo matching errors were reduced considerably. However, it should be noted that the horizontal bias was not corrected (see Figure 9).

The RMSEs of DEMs 1 and 4 were 7.2 and 10.4 m, respectively; the difference was smaller than that generated by the CPs analysis. This is likely to have been because the probability of horizontal error was diminished through the creation of a 5 m DEM, which is 5 times lower than the spatial resolution of KOMPSAT-3 images. It is likely that the automatic bias-compensation method can be applied when generating DEMs with a resolution of 10 m or less.

4.3. Comparative Analysis. We compared the elevation data between DEM 1 and DEM 4 (see colored area in Figure 10(a)). Negative values indicate that DEM 4 overestimated the elevation relative to the DEM 1. Figure 10(b) shows the areas where there are outliers in elevation differences between DEM 1 and DEM 4.

Since the reference DEM and generated DEMs were generated using different methods, comparison of error sources and model characteristics is difficult. The purpose of this study was to determine the possible utility of DEMs generated using various sensor modeling techniques. Comparison among the DEMs produced using common sensor modeling techniques (as in DEM 1) and those based on the automatic bias-compensation method is important. It should be noted that the majority of the study area is covered with

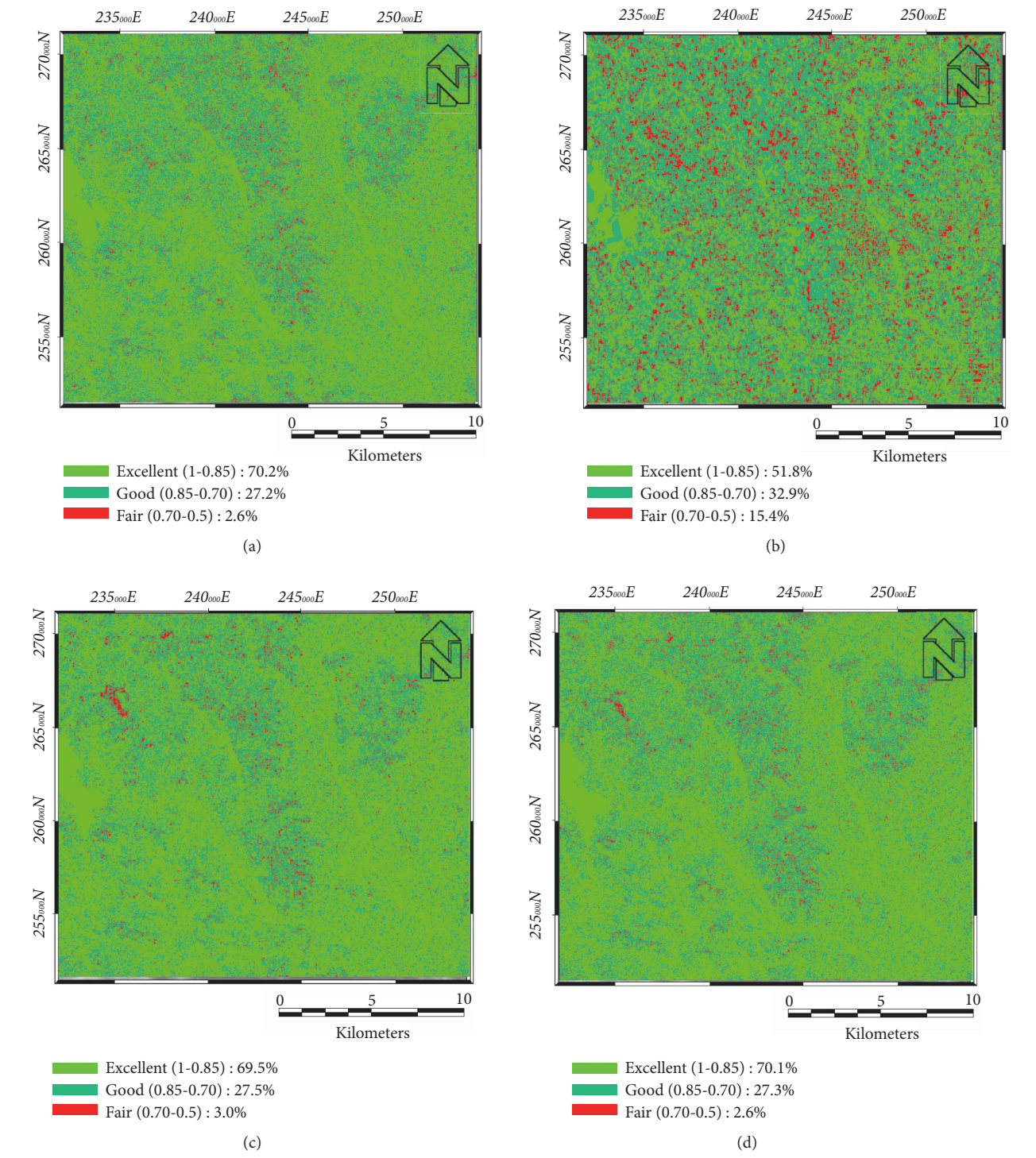

Figure 8: Mass points extraction results: (a) DEM 1, (b) DEM 2, (c) DEM 3, and (d) DEM 4.

forest and, although accurate sensor modeling was achieved, several errors were also present. It is recommended that elevation differences among DEMs be compared over parts of the AOI more likely to be stable, i.e., nonforested areas. For this purpose, AOI DEMs were generated to address an area of around 10 km^2 on the east side of the study area, characterized by few shadows and forest cover. The median elevation difference between AOI DEM 1 and AOI DEM 4 was -1.0 ± 3.4 m (Figure 10(a)).

In the case of mountainous regions, there are several factors that may lead to errors in stereo image matching, including shaded areas that differ by image acquisition time

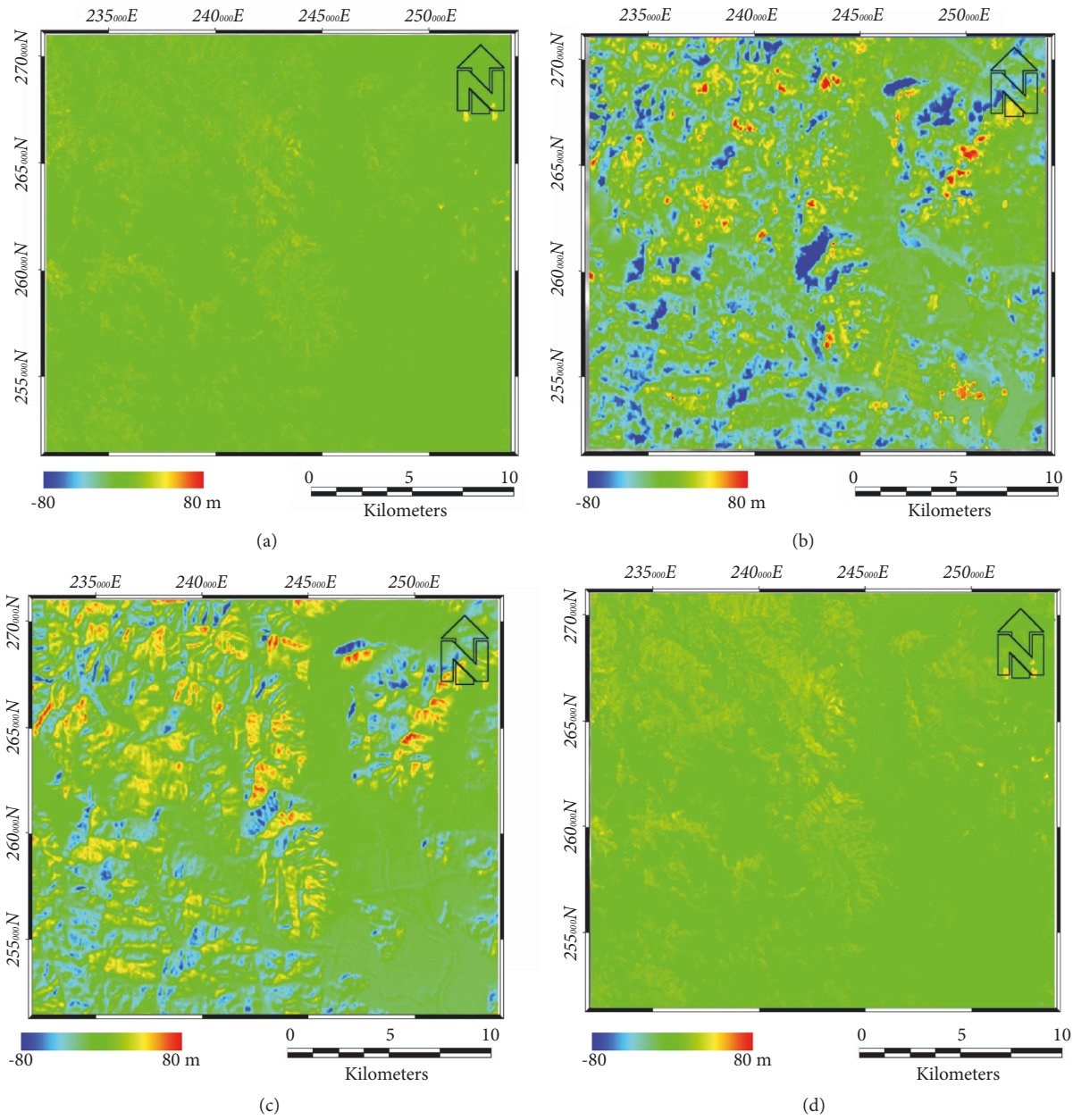

Figure 9: Elevation differences between the reference DEM and (a) DEM 1, (b) DEM 2, (c) DEM 3, and (d) DEM 4.

and direction and the reflection of trees. Accordingly, the mountainous region of the study area generally showed an altitude difference of -5 m to -10 m among the AOI DEMs (Figure 10). In most other areas, accuracy was generally within ± 5 m; however, discrepancies did occur in some urban areas that included man-made structures. Figure 10(b) shows an enlarged image of one such area. Figures 10(c) and 10(d) show enlarged stereo images of the same area.

Figure 10(c) shows a forward image and Figure 10(d) a backward image; the altitude difference among AO DEMs in this area was around -30 m. The error is considered to be due to differences in the shape of, and shadowed area created by, the artificial structure in this area according to the direction in which the image was acquired. Visual inspection showed that most of the discrepancies occurred in forested and shadowed areas. In shadowed regions, textures are more difficult to discern such that image matching performance is poorer, with a bias toward elevation overestimates.

5. Discussion and Conclusion

In this study, we produced four DEMs based on KOMPSAT-3 in-track stereo images and compared their accuracy.

First, we analyzed the stereo geometry of the stereo images acquired by the KOMPSAT-3 and confirmed that all of the factors that can affect accuracy in the horizontal and vertical directions were within the stable range. Second,

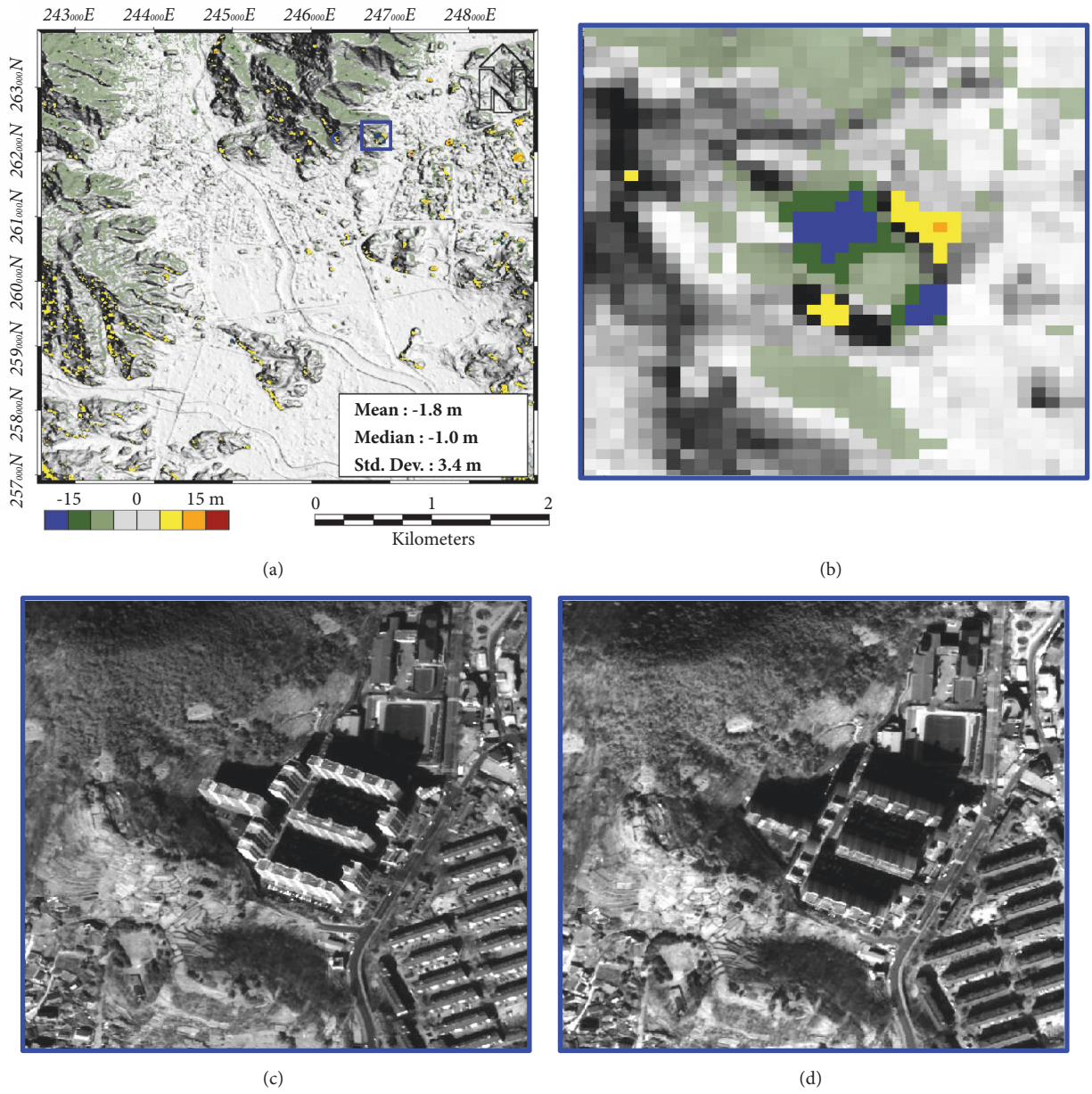

Figure 10: Elevation differences between AOI DEM 1 and AOI DEM 4: (c) and (d) show enlarged stereo images of the region C.

the initial RPCs were corrected to affine correction (DEM 1); the 3D positioning accuracy calculated using 12 CPs was within 3 pixels in the horizontal and vertical directions. Third, when relative adjustment was applied (DEM 3), the percentage of matched points with a correlation of 0.8 or more was improved by at least 17% compared to the case where only initial RPCs were used (DEM 2). Although the absolute horizontal position error of DEM 3 could not be eliminated, the relative elevation error at the same position was significantly reduced. Therefore, if the relative differences in position among DEMs produced at different times can be corrected, they will be able to facilitate the detection of changes in altitude. Finally, when applying the automatic bias-compensated method without GCPs (DEM 4), the percentage of matched points with a correlation of 0.8 or more was 70.1%. When GCPs were used (DEM 1), the value was 70.2%, which was almost the same as the result of DEM 4. The mean difference between DEMs 1 and 4 was -1.8 ± 3.4 m (median, -1.0 m). The results show that DEMs of acceptable quality can be generated without GCPs. Also, although discrepancies among DEMs were noted in forest and shadowed areas, it is possible to generate a 5~10 m resolution DEM with application of additional image processing techniques, such as shadow removal.

Data Availability

The data used to support the finding of this study are available from the corresponding author upon request

Conflicts of Interest

The authors declare that there are no conflicts of interest regarding the publication of this paper.

Acknowledgments

This research was conducted at the Korea Aerospace Research Institute (Grant No. FR19930). The English in this document has been checked by at least two professional editors, both native speakers of English. For a certificate, please see http://www.textcheck.com/certificate/4hRXEE

References

[1] J. H. Oh, D. C. Seo, and C. N. Lee, "A study on DEM generation from Kompsat-3 stereo images," *Journal of the Korean Society of Surveying Geodesy Photogrammetry and Cartography*, vol. 32, no. 1, pp. 19–27, 2014.

[2] S. Rhee, J. Jeong, T. Lee, and T. Kim, "DEM generation from Kompsat-2 images and accuracy comparison by using common software," *Korean Journal of Remote Sensing*, vol. 25, no. 4, pp. 359–366, 2009.

[3] K. H. Chi, K. W. Lee, and N. W. Park, "Landslide stability analysis and prediction modeling with landslide occurrences on KOMPSAT EOC imagery," *Korean Journal of Remote Sensing*, vol. 18, no. 1, pp. 1–12, 2002.

[4] J. Jeong, "Analysis of correlation between geometry elements for the efficient use of satellite stereo images," *Journal of the Korean Society of Surveying, Geodesy, Photogrammetry and Cartography*, vol. 34, no. 5, pp. 471–478, 2016.

[5] K. J. Lee, E. S. Kim, and Y. S. Kim, "Orthorectification of KOMPSAT optical images using various ground reference data and accuracy assessment," *Journal of Sensors*, vol. 2017, Article ID 6393278, 14 pages, 2017.

[6] K. Y. Oh, H. S. Jung, W. J. Lee, and D. T. Lee, "3D geopositioning accuracy assessment using KOMPSAT-2 RPC," *Journal of the Korean Society of Surveying, Geodesy, Photogrammetry and Cartography*, vol. 29, no. 1, pp. 1–9, 2011.

[7] H. Lee, D. Seo, K. Ahn, and D. Jeong, "Positioning accuracy analysis of KOMPSAT-3 satellite imagery by RPC adjustment," *Journal of the Korean Society of Surveying Geodesy Photogrammetry and Cartography*, vol. 31, no. 6, pp. 503–509, 2013.

[8] K.-Y. Oh and H.-S. Jung, "Automated bias-compensation Approach for Pushbroom Sensor Modeling Using Digital Elevation Model," *IEEE Transactions on Geoscience and Remote Sensing*, vol. 54, no. 6, pp. 3400–3409, 2016.

[9] K. Oh, H. Jung, and M. Lee, "Accuracy evaluation of DEM generated from satellite images using automated geo-positioning approach," *Korean Journal of Remote Sensing*, vol. 33, no. 1, pp. 69–77, 2017.

[10] NGII, "National Precision Elevation Model Production Report," 2014.

[11] K. Oh and H. Jung, "Automatic geometric calibration of KOMPSAT-2 stereo pair data," *Korean Journal of Remote Sensing*, vol. 28, no. 2, pp. 191–202, 2012.

[12] S. Ghuffar, "DEM generation from multi satellite planetscope imagery," *Remote Sensing*, vol. 10, no. 9, p. 1462, 2018.

[13] J. H. Oh and C. N. Lee, "Relative RPCs bias-compensation for satellite stereo images processing," *Journal of the Korean Society of Surveying, Geodesy, Photogrammetry and Cartography*, vol. 36, no. 4, pp. 287–293, 2018.

[14] G. Leica Geosystems, "ERDAS field guide: Leica Geosystems GIS & Mapping, LLC," 2014.